Fuzzy Classifier and Bispectrum for Invariant 2-D Shape Recognition

Soowhan Han† and Young-Woon Woo††

ABSTRACT

In this paper, a translation, rotation and scale invariant system for the recognition of closed 2-D images using the bispectrum of a contour sequence and a weighted fuzzy classifier is derived and compared with the recognition process using one of the competitive neural algorithm, called a LVQ(Learning Vector Quantization). The bispectrum based on third order cumulants is applied to the contour sequences of an image to extract fifteen feature vectors for each planar image. These bispectral feature vectors, which are invariant to shape translation, rotation and scale transformation, can be used to the represent two-dimensional planar images and are fed into a weighted fuzzy classifier. The experimental processes with eight different shapes of aircraft images are presented to illustrate a relatively high performance of the proposed recognition system.

2차원 불변 영상 인식을 위한 퍼지 분류기와 바이스펙트럼

한수환† · 우영운††

요 약

이 논문에서는 2차원 영상의 외곽선 정보를 이용하여 추출한 바이스펙트럼과 가중치 퍼지 분류기를 이용하여 영상의 이동, 회전, 크기 변화에 무관한 패턴 인식 기법을 제안하고, 그 인식 결과를 LVQ(Learning Vector Quantization)를 이용한 신경망 분류기와 비교하였다. 3차 큐뮬런트를 근간으로하는 바이스펙트럼은 각 영상의 외각선 정보에 적용되어 15개의 특징값들을 추출한다. 이 특징 벡터들은 영상의 이동, 회전, 크기 변화에 무관한 특징을 가지며 2차원 평면 영상의 대표값으로 사용되어 패턴 분류를 위해 가중치 퍼지 분류기의 입력으로 들어간다. 서로 다른 8가지 비행기들의 평면 영상을 이용하여 실험한 결과들은 제안된 인식 시스템의 성능이 상대적으로 우수함을 보였다.

1. Introduction

The studies on two-dimensional object recognition problem have broad applications such as satellite image identification, the characterization of biomedical images, and the recognition of industrial parts by robots for product assembly. Most of these shape recognition systems require an object to be classified in situations where the position, orientation and distance of the object are time-varying. Additionally, the systems are required to be tolerant to noisy shapes results from the segmentation of objects in varying backgrounds as well as non-ideal imaging conditions. There have been over a dozen prior research efforts to improve the performance of system including Fourier descriptors[1], autoregressive modeling method

† 종신회원, 동의대학교 멀티미디어공학과 조교수
†† 정회원, 동의대학교 컴퓨터공학과 조교수

[2]-[4], dynamic alignment process of contour sequences[5], and neural network approach[6]-[10].

The accuracy on pattern recognition problems, while keeping simplicity of the overall system, depends on two important factors. One is to extract feature vectors representing a 2-D object image. The feature vectors should have a small dimensionality for real-time process, a similarity between intraclasses. In this study, the boundary of a closed planar shape is characterized by an ordered sequence that represents the Euclidean distance between the centroid and all boundary pixels since the overall shape information is contained in the boundary of the shape. The amplitude of this ordered sequence is invariant to translation because the Euclidean distance with the same starting boundary pixel remains unchanged even an image is shifted. Then, the contour sequence is normalized with respect to the size of image. This normalization includes the amplitude and the duration of the contour sequence. Next the bispectrum based on third order cumulants is applied to this normalized contour sequence as a means of feature selection. Higher order spectra (bispectrum, trispectrum) play an important role in digital signal processing due to their ability of preserving nonminimum phase information, as well as information due to deviations from Gaussianity and degrees of nonlinearities in time series[11]. In the last few years, bispectral analysis has been an active research area. The applications of the bispectrum extend over several disciplines. These applications include ARMA modeling, analysis of bilinear models, detection of phase coupling, signal reconstruction, image processing, radar signal detection, and so on [12]-[14]. In the previous works for recognition systems [8]-[9], the spectrum feature vectors were extracted from power spectrum density of contour sequence. However, the power spectrum of contour sequence is corrupted by white gaussian noise power $E[n^2] = \delta_n^2$ in the all frequency components where the bispectrum is not. The reason for that will be shown in next section and Han's work presents that the bispectral feature vector has a better noisy tolerant characteristic[10]. Therefore, in this investigation of 2-D object classification, the bispectral components of the normalized contour sequence of an object image are utilized as feature vectors. These bispectral feature vectors have enough shape information to represent each 2-D object, a property to be invariant in size, shift, and rotation, and are used as the input of fuzzy classifier.

Another factor is to select an appropriate classifier architecture for this particular recognition task. In a recent year, the neural network algorithms[8]-[10] and the fuzzy memberships functions [15][16] are widely used. However, the hybrid neural structure with back-propagation and counter-propagation in [8] and with two fuzzy ART modules is relatively complicated, and the fuzzy ARTMAP in [9] had used the *five*-voting strategy (repeat five simulations with different ordering of training patterns) to avoid the ordering influence of training patterns. Moreover it is hard to select an optimal matching of specific neural network architecture for this kind of recognition system among many different neural models. Thus, a triangular fuzzy membership function and a weighted fuzzy mean are utilized as a classifier. This fuzzy classifier has a simple structure and it can easily improve the classification results by a weighted fuzzy mean extracted from analyzing the bispectral feature vectors. In the experimental procedure, the proposed fuzzy classifier is tested with eight different shapes of aircraft images and compared with the results of the previous work[10] using a LVQ, one of the competitive neural classifiers.

2. Shape Information and Bispectral Feature Extraction

In this portion of the study, the boundary of a

closed planar shape is characterized by an ordered sequence that represents the Euclidean distance between the centroid and all contour pixels of the digitized shape. Clearly, this ordered sequence carries the essential shape information of a closed planar image. The bispectral feature extraction from a closed planar image is done as follows. First, the boundary pixels are extracted by using contour following algorithm and the centroid is derived[17][18]. The second step is to obtain an ordered sequence in a clockwise direction, b(i), that represents the Euclidean distance between the centroid and all boundary pixels. Since only closed contours are considered, the resulting sequential representation is periodic as shown in equation (1).

$$b(i)=\sqrt{(x_i-x_c)^2+(y_i-y_c)^2}$$
$$b(N+i)=b(i) \quad i=1,2,3,......,N \tag{1}$$

where (x_c, y_c) : the centroid of an image, (x_i, y_i) : the contour pixel, N(period) : the total number of boundary pixels.

This Euclidean distance remains unchanged to a shift in the position of original image. Thus the sequence $b(i)$ is invariant to translation. The next step is to normalize the contour sequence with respect to the size of image. Scaling a shape results is the scaling of the samples and duration of the contour sequence. Thus the scale normalization involves both an amplitude and a duration normalization. The normalized duration of the sequence, 256 points fixed, is obtained by resampling operation and function approximation. This is shown in equation (2).

$$c(k)=b(k*N/256) \quad k=1,2,3......,256 \tag{2}$$

where N is the total number of boundary pixels.

After duration normalization, amplitude is divided by sum of contour sequence and subtracted the mean. It is shown in equation (3) and (4).

$$d(k)=c(k)/s \quad k=1,2,3,.....,256 \tag{3}$$

$$d(k)=d(k)-mean(d(k)) \tag{4}$$
$$where\ s=c(1)+c(2)+c(3)+.......+c(256)$$

This sequence $d(k)$ is invariant to translation and scaling. In a forth, the bispectral feature measurement is taken into the contour sequence. The spectral density of the sequence $d(k)$ utilized in this paper is a third-order spectrum, called a bispectrum. In general, the higher-order spectra can address noise suppression, and preserve non-minimum phase information as well as the information due to degrees of nonlinearities[19]. Thus, it has been widely used in the area of the identification of nonminimum phase systems, detection of phase coupling and ARMA modeling[20][21]. In this study to 2-D shape recognition, the bispectrum of contour sequence $d(k)$, instead of power spectrum, is investigated for feature vectors because of its better noisy-tolerant characteristic [10][19]. The nth order cumulants spectrum of contour sequence d(k) is defined as

$$\begin{aligned} &H_n(\omega_1, \cdots, \omega_{n-1}) \\ &= \frac{1}{(2\pi)^{n-1}} \sum_{\tau_1=-\infty}^{+\infty} \cdots \sum_{\tau_{n-1}=-\infty}^{+\infty} C_d(\tau_1, \cdots, \tau_{n-1}) e^{-j(w_1\tau_1+w_2\tau_2+\ldots+w_n\tau_n)} \\ &= F(\omega_1)\cdots F(\omega_{n-1})F^*(\omega_1+\cdots+\omega_{n-1}) \end{aligned} \tag{5}$$

where C_d and F are cumulants and Fourier transform of the sequence $d(k)$, respectively. For the special cases where n=2(power spectrum) and n=3 (bispectrum) :

$$\begin{aligned} H_2(\omega) &= \frac{1}{2\pi} \sum_{\tau=-\infty}^{\infty} C_d(\tau) e^{-j\omega\tau} \\ &= \frac{1}{2\pi} \sum_{\tau=-\infty}^{\infty} \frac{1}{2\pi} \sum_{k=-\infty}^{\infty} d(k)d(k+\tau) e^{-j\omega\tau} \\ &= \frac{1}{2\pi} \sum_{\tau=-\infty}^{\infty} \frac{1}{2\pi} \sum_{k=-\infty}^{\infty} d(k)d(k+\tau) e^{-j\omega(k+\tau-k)} \\ &= \frac{1}{2\pi} \sum_{\tau=-\infty}^{\infty} d(k+\tau) e^{-j\omega(k+\tau)} \\ &\quad \cdot \frac{1}{2\pi} \sum_{k=-\infty}^{\infty} d(k) e^{j\omega k} \\ &= F(\omega)F^*(\omega) \end{aligned} \tag{6}$$

where $C_d(\tau)=E[d(k)d(k+\tau)]$: Expectation of

$d(k)d(k+\tau)$.

$$
\begin{aligned}
&H_3(\omega_1, \omega_2) \\
&= \frac{1}{(2\pi)^2} \sum_{\tau_1=-\infty}^{+\infty} \sum_{\tau_2=-\infty}^{+\infty} C_d(\tau_1, \tau_2) e^{-j(\omega_1\tau_1+\omega_2\tau_2)} \\
&= \frac{1}{(2\pi)^2} \sum_{\tau_1=-\infty}^{+\infty} \sum_{\tau_2=-\infty}^{+\infty} \\
&\quad \frac{1}{2\pi} \sum_{k=-\infty}^{+\infty} d(k)d(k+\tau_1)d(k+\tau_2) e^{-j(\omega_1\tau_1+\omega_2\tau_2)} \\
&= \frac{1}{(2\pi)^2} \sum_{\tau_1=-\infty}^{+\infty} \sum_{\tau_2=-\infty}^{+\infty} \\
&\quad \frac{1}{2\pi} \sum_{k=-\infty}^{+\infty} d(k)d(k+\tau_1)d(k+\tau_2) \\
&\qquad \cdot e^{-j[\omega_1(k+\tau_1)+\omega_2(k+\tau_2)-k(\omega_1+\omega_2)]} \\
&= \frac{1}{2\pi} \sum_{\tau_1=-\infty}^{+\infty} d(k+\tau_1) e^{-j\omega_1(\tau_1+k)} \\
&\quad \cdot \frac{1}{2\pi} \sum_{\tau_2=-\infty}^{+\infty} d(k+\tau_2) e^{-j\omega_2(\tau_2+k)} \\
&\quad \cdot \frac{1}{2\pi} \sum_{k=-\infty}^{+\infty} d(k) e^{j(\omega_1+\omega_2)k} \qquad (7) \\
&= F(\omega_1)F(\omega_2)F^*(\omega_1+\omega_2)
\end{aligned}
$$

where $C_d(\tau_1, \tau_2) = E[d(k)d(k+\tau_1)d(k+\tau_2)]$ and $|\omega_1| \le \pi$, $|\omega_2| \le \pi$, $|\omega_1+\omega_2| \le \pi$.

If the observed contour sequence *d(k)=s(k)+n(k)* where *s(k)*: the zero mean contour sequence without noise, *n(k)*: the zero mean white gaussian noise sequence and they are independent, equations (6) and (7) becomes

$$
\begin{aligned}
&H_2(\omega) \\
&= \frac{1}{2\pi} \sum_{\tau=-\infty}^{+\infty} C_s(\tau) e^{-j\omega\tau} + \frac{1}{2\pi} \sum_{\tau=-\infty}^{+\infty} C_n(\tau) e^{-j\omega\tau} \qquad (8) \\
&= H_s(\omega) + H_n(\omega) \qquad (9) \\
&= H_s(\omega) + \frac{1}{2\pi}\left(\frac{N_0}{2}\right)
\end{aligned}
$$

where $C_s(\tau) = E[s(k)s(k+\tau)]$ and

$$C_n(\tau) = E[n(k)n(k+\tau)] = \frac{N_0}{2}\delta(\tau).$$

$$
\begin{aligned}
&H_3(\omega_1, \omega_2) \\
&= \frac{1}{(2\pi)^2} \sum_{\tau_1=-\infty}^{\infty} \sum_{\tau_2=-\infty}^{\infty} C_s(\tau_1, \tau_2) e^{-j(\omega_1\tau_1+\omega_2\tau_2)} \\
&\quad + \frac{1}{(2\pi)^2} \sum_{\tau_1=-\infty}^{\infty} \sum_{\tau_2=-\infty}^{\infty} C_n(\tau_1, \tau_2) e^{-j(\omega_1\tau_1+\omega_2\tau_2)} \qquad (10) \\
&= H_s(\omega_1, \omega_2) + H_n(\omega_1, \omega_2) \\
&= H_s(\omega_1, \omega_2) + \gamma_n \\
&= H_s(\omega_1, \omega_2) + E[n^3(k)] \qquad (11)
\end{aligned}
$$

where $C_s(\tau_1, \tau_2) = E[s(k)s(k+\tau_1)s(k+\tau_2)]$ and $C_n(\tau_1, \tau_2) = E[n(k)n(k+\tau_1)n(k+\tau_2)] = \gamma_n\delta(\tau_1, \tau_2)$

In equation (11), the noisy bispectrum $H_n = E[n(k)^3] = \gamma_n$ becomes zero because of skewness of noisy density function, which means the bispectrum suppress the white noisy portion and the extracted feature vectors have better noisy tolerance than the feature vectors from the power spectrum. The performance comparisons with noise for robust 2-D shape recognitions between the power spectral and the bispectral features are shown in [10]. And trispectrum with cumulants order n=4 contains the noisy spectrum because of kurtosis of noisy density and the higher spectra with cumulant order more than n=4 have not widely used yet because of their computational complexity and the difficulty of feature extraction from n-dimensional spectrum space. Therefore the bispectrum is utilized for feature selection of 2-D shape images in this paper.

The magnitude of bispectrum derived in a forth step, $|H_3(\omega_1, \omega_2)|$, is unchanged even after the sequence d(k) is circular shifted because the magnitude of Fourier transform, $|F(\omega)|$, is not changed[22]. Thus $|H_3(\omega_1, \omega_2)|$ is invariant to the rotation of an image. Finally, the two dimensional bispectral magnitude (256 by 256) is projected to vertical axis (ω_1) by taking mean value of each column for feature extraction. It is shown in equation (12).

h[k]=[mean(*kth* column of $|H_3(\omega_1, \omega_2)|$)] (12)

where k=1,2,....256.

The first column and the row in the magnitude of bispectrum contain all zero value because the

normalized contour sequence has a zero mean. It means h(1) is always zero. And the projected bispectral components exceed to the sixteenth have very small values (near zero). Thus, for fast recognition process with reliable accuracy, the projected bispectral components from the second to the sixteenth (h(2), h(3),.....h(16)) are chosen to be used as feature vectors to represent each image shape, which are fed into a proposed fuzzy logic classifier for recognition process. The overall bispectral feature extraction process is shown in Fig. 1.

(a) Reference image

↓
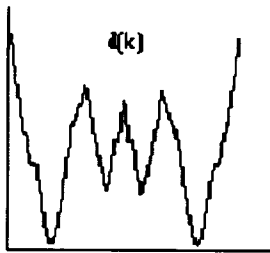
(b) Size & duration normalized contour sequence *d(k)* (x axis : contour sequences, y axis : distance)

↓
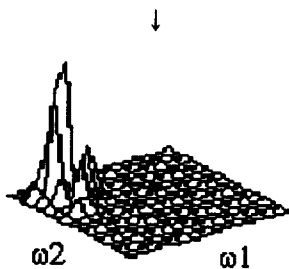
(c) Bispectrum magnitude(upper left coner:16 by 16) of contour sequence *d(k)*

↓
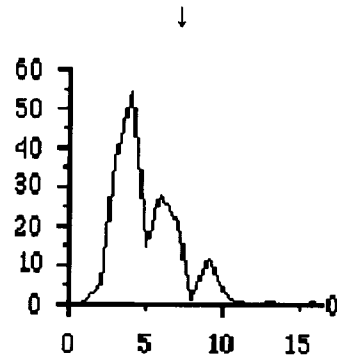
(d) Fifteen bispectral feature vectors obtained by vertical projection: *h(2), h(3), ..., h(16)* (x axis : number of sequences, y axis : bispectral amplitude after projection)

Fig. 1. The overall bispectral feature extraction process.

These feature vectors have the desired format for planar image recognition system, which means they are invariant to translation, rotation and scaling of the shape and highly tolerant to the noise. Fig. 2, 3 and 4 show the fifteen projected bispectral feature vectors of rotated image, two different shapes and 10dB noisy image.
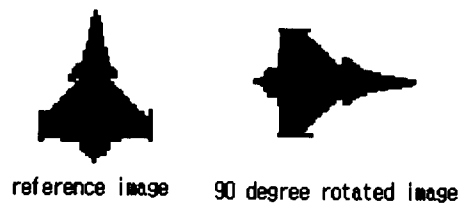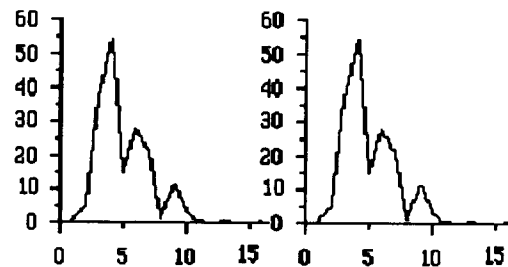
Fig. 2. Bispectral feature vectors extracted from reference and rotated images.
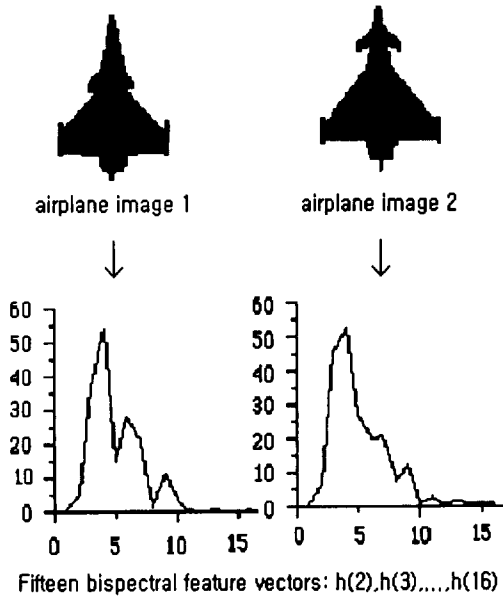
Fig. 3. Bispectral feature vectors extracted from two different images.
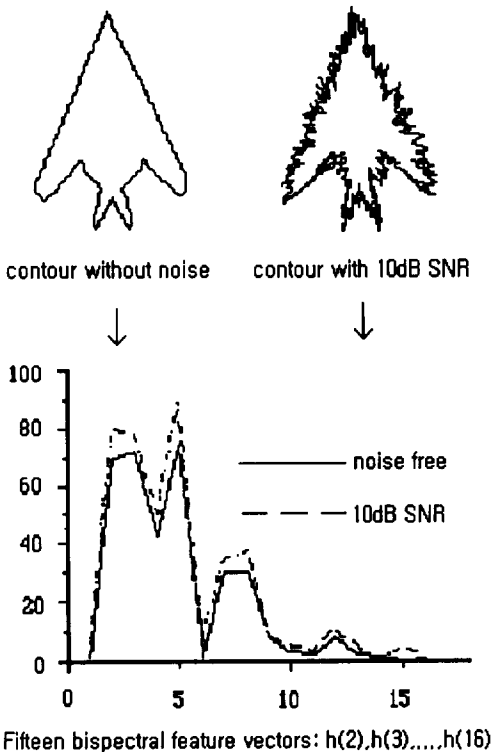
Fig. 4. Bispectral feature vectors extracted from the contour images without noise and with 10dB SNR.

3. Fuzzy Classifier Using Weighted Fuzzy Mean

There are various methods to construct the fuzzy classifier depending on the type of fuzzy membership function and the calculation method of mean value for membership grades[16]. The two of most popular types for fuzzy membership function are triangle shown in Fig. 5 and trapezoid shown in Fig. 6[23]. And the arithmetic mean written in equation (13), the harmonic mean in equation (14) and the weighted mean in equation (15) are widely used for the calculation of mean value[24].
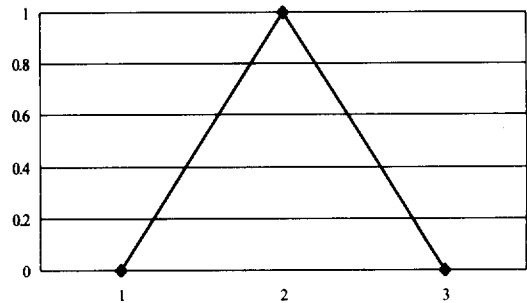
Fig. 5. An example of triangular form of a fuzzy membership function.
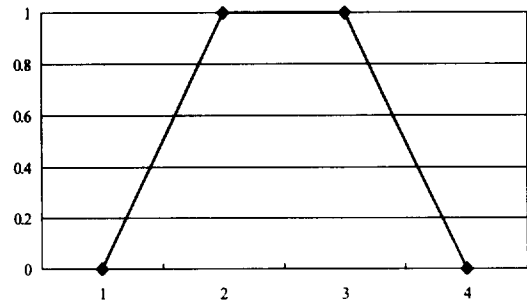
Fig. 6. An example of trapezoid form of a fuzzy membership function.

$$h_1(\mu_1(x), \mu_2(x), \ldots, \mu_n(x)) = \frac{1}{n}\sum_{i=1}^{n}\mu_i(x) \qquad (13)$$

$$h_{-1}(\mu_1(x), \mu_2(x), \ldots, \mu_n(x)) = \frac{n}{\sum_{i=1}^{n}\frac{1}{\mu_i(x)}} \qquad (14)$$

$$h_w(\mu_1(x), \mu_2(x), \ldots, \mu_n(x); w_1, w_2, \ldots, w_n) = \sum_{i=1}^{n} \mu_i(x) \cdot w_i \, , \quad (\sum_{i=1}^{n} w_i = 1) \tag{15}$$

where μ_i is an ith membership grade, w_i is an ith weight and n is the number of fuzzy membership functions.

The proposed fuzzy classifier in this work uses the triangular type of fuzzy membership function and the weighted fuzzy mean method whose variance is utilized for weights. The triangular type of fuzzy membership functions is useful where the only one reference feature set is available as in this study. The one of advantage of the proposed fuzzy classifier is not required the training stage unlike the neual network structure. Only 120 fuzzy membership functions (15×8: the one membership function for each of fifteen dimensional feature values × the eight reference aircraft images) and 15 variances for each dimensional value of feature vector are established for classification process. This preprocessing step is much faster and easier than that of the conventional training stage of neural classifier. Another advantage of this fuzzy classifier is the use of a variance as a weight. In general, it is hard for the neural classifiers to improve the performance results because they are highly depend on the architectures, learning algorithm and training order[9][25]. However, the improvement of recognition results for the fuzzy classifier is easily achieved with the variance extracted from analyzing the characteristics of the bispectral feature vectors. That is shown in next section. Therefore the triangular fuzzy membership function and the weighted fuzzy mean method with variance are utilized as a fuzzy classifier.

4. Experimental Results and Performance Assessment

The methodology presented in this paper, for the recognition of closed planar shape, was evaluated with eight different shapes of aircraft. They are shown in Fig. 7.
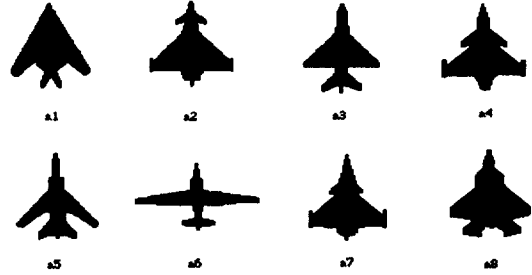
Fig. 7. Eight different shapes of reference aircraft images.

From each reference shape of aircraft, 36 noisy-free patterns were generated by rotating the original image with 30 degree increment and scaling with three factor (1, 0.8 and 0,6). And forty noisy corrupted patterns were made by adding four different level of random gaussian noise (25dB, 20dB, 15dB, 10dB SNR : ten noisy patterns for each SNR) to 36 noisy-free patterns. Thus the data set for each reference aircraft image has 36 noisy-free patterns and 1440 (40×36) noisy corrupted patterns. The number of total test patterns becomes 11808 (1476×8 reference image). The sample contour images for a4 and a7 with noise-free and with 10dB SNR are shown in Fig. 8.

The construction of a fuzzy classifier and the recognition process are done by as follows. First, the fifteen fuzzy membership functions for each reference aircraft image are established by using each of the fifteen dimensional bispectral feature values. The fuzzy membership functions are defined by equation (16).

$$\begin{aligned} y_{ij} &= 0.01 \cdot (x_{ij-f_{ij}}) + 1 \quad (-100 + f_{ij} < x_{ij} < f_{ij}), \\ y_{ij} &= -0.01 \cdot (x_{ij} - f_{ij}) + 1 \quad (f_{ij} < x_{ij} < 100 + f_{ij}), \end{aligned} \tag{16}$$

otherwise $y_{ij} = 0$
(*where* $i = 1 \sim 8, \; j = 1 \sim 15$)

where 0.01 is the slope of a fuzzy membership functions, x_{ij} is an input value for the jth feature of the aircraft image ai, f_{ij} is an reference value for the jth feature of the aircraft image ai and y_{ij} is an membership grade for x_{ij}..

All of membership functions are configured as a triangular type shown in Fig. 9. The number of total fuzzy membership functions becomes 120 for the eight different type of aircraft images.
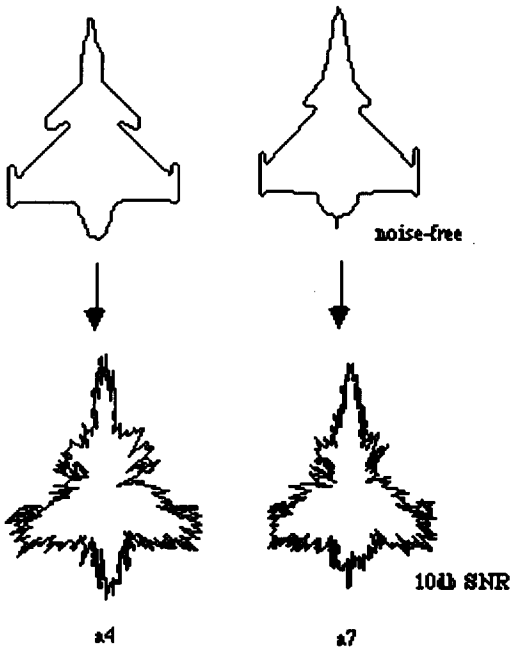
Fig. 8. The sample contour images for a4 and a7 with noise-free and with 10dB SNR.
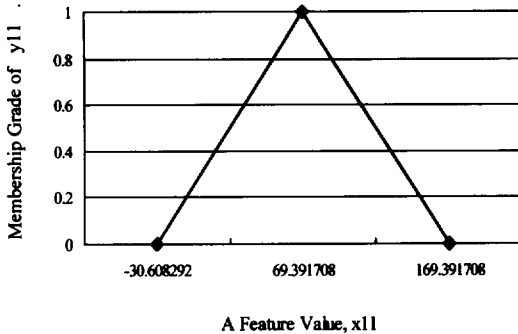
Fig. 9. The fuzzy membership function, y11 extracted from the first feature value, f11 for an aircraft image, a1 (f11= 69.391708).

In a second step, the variances for each of the normalized fifteen dimensional feature values with eight reference aircraft images are derived by equation (17) and (18). The normalized feature values from reference aircraft a1 to a8 are shown in Fig. 10. Those variances are utilized as the weights for recognition process.

$$m_j = \frac{1}{8}\sum_{i=1}^{8} x_{ij} \quad (j=1..15) \tag{17}$$

where m_j is a mean of jth feature values for the eight different aircraft images and x_{ij} is a jth feature value for aircraft image ai.

$$vr_j = \frac{1}{8}\sum_{i=1}^{8}(x_{ij}-m_j)^2 \quad (j=1..15) \tag{18}$$

where vr_j is a variance of jth feature values for the eight different aircraft images(a1,a2,...,a8).

In the third, the fifteen bispectral feature values of the incoming test aircraft image are applied to the corresponding fuzzy membership function for each of eight reference shapes and the membership grades are computed by equation (16). The fifteen membership grades for any one of eight reference shapes present the degree of similarity with that reference shape.

Finally the weighted mean values of the membership grades for each of eight reference aircraft shape are computed by equation (19) and (20), and a reference shape of aircraft image having the largest weighted mean value (the largest h_i) is chosen as a recognition result.

$$w_j = vr_j \quad (j=1..15) \tag{19}$$

where w_j is a weight for the jth feature value.

$$h_i(y_{i1}(x_{i1}), y_{i2}(x_{i2}), \ldots, y_{i15}(x_{i15}); w_1, w_2, \ldots, w_{15}) = \sum_{j=1}^{15} y_{ij}(x_{ij}) \cdot w_j\ , \quad (i=1..8) \tag{20}$$

where y_{ij} is an membership grade for the jth feature value of the aircraft image ai computed by equation (16), and h_i is a weighted fuzzy mean value for each of eight reference aircraft images.
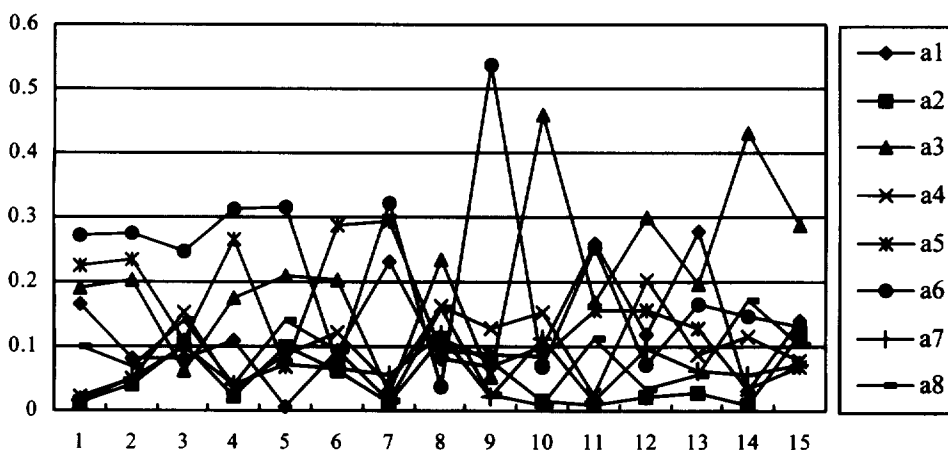
Fig. 10. Normalized amplitudes of bispectral features.

The experimental process was performed under six different experimental environments. The experiments of 2, 4, and 6 are performed by the proposed fuzzy classifier and the others are performed by the neural classifier, a LVQ, used in previous work[10]. These are as follows.

Experiment 1.

Neural classifier algorithm : LVQ1 with 8 output clusters (one cluster for each reference shape).

Training data set : only the 8 reference aircraft images.

Experiment 2.

Classifier algorithm : the weighted fuzzy mean using variance.

Reference data set for membership function: same as training data set of experiment 1.

Experiment 3.

Classifier algorithm : LVQ1 with 8 output clusters (one cluster for each reference shape).

Training data set : 8 reference patterns + 32 noisy patterns (4 noisy patterns with 25dB SNR generated from each of 8 reference images).

Experiment 4.

Classifier algorithm : same as 2.

Reference data set for membership function: average of training data set of experiment 3.

Experiment 5.

Neural classifier algorithm : an improved LVQ algorithm called LVQ3 with 16 output clusters (two clusters for each reference shape).

Training data set : 8 reference patterns + 32 noisy patterns (4 noisy patterns with each of 25dB, 20dB, 15dB and 10dB SNR generated from each of 8 reference images).

Experiment 6.

Classifier algorithm : same as 2.

Reference data set for membership function: average of training data set of experiment 5.

Under each of six different experimental environments, 11808 of total test patterns (1476 patterns for each reference image) were evaluated. The overall classification results of experiments 1-6 are summarized in table 1 and 2. In table 1, the best results of a proposed fuzzy classifier are compared with the best results of a LVQ neural classifier. In experiments of 4 and 6 for a fuzzy classifier, the membership functions for each of eight reference shapes are constructed with a noise-free pattern and four of randomly selected

Table 1. Comparison of the classification performance using best results.

	Experiment 1 (LVQ1)	Experiment 2 (Weighted Fuzzy Mean)	Experiment 3 (LVQ1)	Experiment 4 (Weighted Fuzzy Mean)	Experiment 5 (LVQ3)	Experiment 6 (Weighted Fuzzy Mean)
Noise-free	288/288 (100%)	288/288 (100%)	288/288 (100%)	288/288 (100%)	288/288 (100%)	288/288 (100%)
25dB	2880/2880 (100%)	2880/2880 (100%)	2880/2880 (100%)	2880/2880 (100%)	2880/2880 (100%)	2880/2880 (100%)
20dB	2880/2880 (100%)	2880/2880 (100%)	2880/2880 (100%)	2880/2880 (100%)	2880/2880 (100%)	2880/2880 (100%)
15dB	2880/2880 (100%)	2880/2880 (100%)	2880/2880 (100%)	2880/2880 (100%)	2880/2880 (100%)	2880/2880 (100%)
10dB	2765/2880 (96.01%)	2806/2880 (97.43%)	2776/2880 (96.39%)	2821/2880 (97.95%)	2871/2880 (99.69%)	2868/2880 (99.58%)
Total # of correctly classified patterns(%)	11693/11808 (99.03%)	11732/11808 (99.37%)	11704/11808 (99.12%)	11749/11808 (99.50%)	11799/11808 (99.92%)	11796/11808 (99.90%)

Table 2. The averaged classification results (Other cases are same as in table 1)

	Exp. 3 (LVQ1)	Exp. 4 (WFM)	Exp. 5 (LVQ3)	Exp. 6 (WFM)
10dB	2767/2880 (96.08%)	2814/2880 (97.71%)	2852/2880 (99.03%)	2859/2880 (99.27%)
Total # of correctly classified patterns(%)	11695 /11808 (99.04%)	11742 /11808 (99.44%)	11780 /11808 (99.76%)	11787 /11808 (99.82%)

noisy patterns. It means the classification results slightly depend on the selection of noisy patterns. By the same case, in experiments of 3 and 5 for a LVQ classifier, the classification results depend on the selection of noisy patterns for training. Therefore the five independent simulations with different styles of noisy patterns keeping the same SNR were evaluated and the results were averaged. Those are shown in table 2.

The classification results with both of a LVQ and a fuzzy classifier can be increased by adding some noisy patterns to training process and to construction of membership function, respectively. These are shown in the results of experiment 1, 3 and 5 with the LVQ neural classifier and in the results of experiment 2, 4 and 6 with the proposed fuzzy classifier. And table 1 and 2 show that both classifiers perform well to recognize the eight different shapes of images where the signal power is relatively larger than the noise power. However, the experimental results of 1, 2, 3, and 4 with 10dB SNR show that a LVQ neural classifier is more easily affected by noise. It means that the fuzzy classifier measuring the weighted fuzzy mean is more effective than a LVQ measuring the Euclidean distance where the images are highly corrupted by noise. And the structure and learning algorithm of LVQ3 used in experiment 5 are more complicated than those of LVQ1 and this proposed fuzzy classifier even the performance result is not significantly different with a result of experiment 6.

5. Conclusion

The high recognition results including the performance comparison with a LVQ show that the weighted fuzzy classifier with the fifteen bispectral feature vectors extracted from the normalized contour sequences of planar shapes, performs well to recognize the different shapes of aircraft even the aircraft images are rotated, scaled and significantly corrupted by noise. Additionally, the

fuzzy classifier can easily improve the recognition results by analyzing the incoming feature vectors and also it does not require the training stage as the neural network classifier does.

In a near future, more realistic data such as the satellite images or the biomedical images will be tested and investigated for the practical applications. At the same time, the way to segment the shape of image from noisy background should be considered.

References

[1] C. C. Lin and R. Chellappa, "Classification of partial 2-D shapes using Fourier descriptors," *IEEE Trans. on PAMI*, Vol. 9, No. 5, pp. 686-690, Sep., 1987.

[2] S.R. Dubois and F.H. Glanz, "Autoregressive Model Approach to Two-Dimensional Shape Classification," *IEEE Trans. on PAMI*, Vol. 8, No. 1, Jan., 1986

[3] I. Sekita, T. Kurita, and N. Otsu, "Complex Autoregressive Model for Shape Recognition," *IEEE Trans. on PAMI*, Vol. 14, No. 4, April 1992.

[4] M. Das, M. J. Paulik, and N. K. Loh, "A Bivariate Autoregressive Modeling Technique for Analysis and Classification of Planar Shapes," *IEEE Trans. on PAMI*, Vol. 12, No. 1, Jan., 1990.

[5] L. Gupta and M. D. Srinath, "Invariant Planar Shape Recognition Using Dynamic Alignment," *Pattern Recognition*, Vol.21, No. 3, pp. 235-239, 1988.

[6] L. Gupta and M.R. Sayeh and R. Tammana, "A neural network approach to robust shape classification," *Pattern Recognition*, Vol. 23, No. 6, pp. 563-568, 1990.

[7] Lilly and M. B. Reid, "Robust position, scale, and rotation invariant object recognition using higher-order neural networks," *Pattern Recognition*, Vol. 25, No. 9, pp. 975-985, 1992.

[8] B. H. Cho, "Rotation, translation adn scale invariant 2-D object recognition using spectral analysis and a hybrid neural network," *Florida Institute of Technology*, Melbourne, Florida, U.S.A., Ph.D. Thesis 1993.

[9] S.W. Han, "Robust Planar Shape Recognition Using Spectrum Analyzer and Fuzzy ARTMAP," *Journal of Fuzzy Logic and Intelligent Systems*, Vol 5, No. 4, pp. 33-40, June, 1997.

[10] S. W.Han, "A Study on 2-D Shape Recognition Using Higher-Order Spectral and LVQ," *Journal of Fuzzy Logic and Intelligent Systems*, Vol 9 No. 3 pp. 285-293, 1999.

[11] C. L. Nikias and M. R. Raghuveer, "Bispectrum estimation : A digital signal processing framework," *Proc. IEEE*, Vol. 75, No. 7, pp. 869-891, July, 1987.

[12] T. Erdem and M. Tekalp, "Linear Bispectrum of Signals and Identification of Nonminimum Phase FIR Systems Driven by Colored Input," *IEEE Trans. Signal Processing*, Vol 40, No. 6, pp. 1469-1479, 1992.

[13] I. Jouny, "Description of radar targets using the bispectrum," *IEEE Proc.-Radar, Sonar Navig.*, Vol. 141, No. 3, pp. 159-163, 1994.

[14] E. K. Walton and I. Jouny, "Bispectral analysis of radar signature and application to target classification," *Radio Sci.*, Vol. 25, pp. 101-113, 1990.

[15] A. Kandel, *Fuzzy Techniques in Pattern Recognition*, John Wiley & Sons, Inc., pp. 91-127, 1982.

[16] H. -J, Zimmermann, *Fuzzy Set Theory - and Its Applications*, Kluwer Academic Publishers, pp. 217-239, 1996.

[17] R. C. Gonzalez adn R. E. Woods, *Digital Image Processing*, Addison-Wesley Publishing Company, Inc., pp. 391-395, 1992.

[18] W. K. Pratt, *Digital Image Processing, 2nd ed.*, Wiley Interscience, pp. 623-625, 1991.

[19] C. L. Nikias and J. M. Mendel, *Signal Processing with Higher-Order Spectra*, United

Signals & Systems, Inc., pp. 12-37, 1990.

[20] J.K. Tugnait, "Identification of nonminimum phase linear stochastic system," *Automatica*, Vol. 22, pp. 457-464, July 1986.

[21] C. L. Nikias, "ARMA bispectrum approach to nonminium phase system identification," *IEEE Trans. Acoust., Speech, Signal Processing*, Vol.36, pp. 513-524, April 1988.

[22] A. V. Oppenheim and R.W. Schafer, *Digital Signal Processing*, Prentice-Hall, N.J., pp. 101-110, 1975.

[23] D. Dubois and H. Prade, *Fuzzy Sets and Systems*, Academic Press, New York, pp. 95-106, 1980.

[24] G. J. Klir and T. A. Folger, *Fuzzy Sets, Uncertainty, and Information*, Prentice Hall, New Jersey, pp. 58-61, 1988.

[25] L. Fausett, *Fundamentals of Neural Networks : Architectures, Alogrithm, and Applications*, Prentice Hall, pp. 176-195, 1994.

한 수 환

1986년 2월 연세대학교 전자공학과 졸업(공학사)
1990년 3월 미 Florida Institute of Technology 전기전자공학과 졸업(공학석사)
1993년 6월 미 Florida Institute of Technology 전기전자공학과 졸업(공학박사)
1994년 3월~1997년 2월 관동대학교 전자계산공학과 조교수
1997년 3월~현재 동의대학교 멀티미디어공학과 조교수
관심분야 : Digital Signal & Image Processing, Pattern Recognition, Fuzzy Longic and Neural Networks
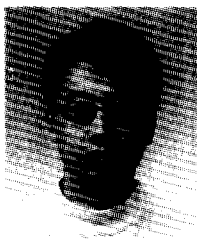
우 영 운

1967년 2월생
1989년 연세대학교 전자공학과 졸업(공학사)
1991년 연세대학교 본대학원 전자공학과 졸업(공학석사)
1997년 연세대학교 본대학원 전자공학과 졸업(공학박사)
1997년~현재 동의대학교 컴퓨터공학과 조교수
관심분야 : 전문가 시스템, 패턴 인식, 인공 지능